ORIGINAL RESEARCH

Systemic delivery of the anticancer agent arenobufagin using polymeric nanomicelles

Xue Yuan[1,2]
Qian Xie[1]
Keyu Su[1]
Zhijie Li[3]
Dong Dong[3]
Baojian Wu[1,2]

[1]Research Center for Biopharmaceutics and Pharmacokinetics, College of Pharmacy, [2]Guangdong Province Key Laboratory of Pharmacodynamic Constituents of TCM and New Drugs Research, [3]International Ocular Surface Research Centre and Institute of Ophthalmology, School of Medicine, Jinan University, Guangzhou, China

Correspondence: Baojian Wu
College of Pharmacy, Jinan University, 601 Huangpu Avenue West, Guangzhou, China
Email bj.wu@hotmail.com

Dong Dong
School of Medicine, Jinan University, 601 Huangpu Avenue West, Guangzhou, China
Email dongdong1983jd@163.com

Abstract: Arenobufagin (ABG) is a major active component of toad venom, a traditional Chinese medicine used for cancer therapy. However, poor aqueous solubility limits its pharmacological studies in vivo due to administration difficulties. In this study, we aimed to develop a polymeric nanomicelle (PN) system to enhance the solubility of ABG for effective intravenous delivery. ABG-loaded PNs (ABG-PNs) were prepared with methoxy poly (ethylene glycol)-block-poly (D,L-lactic-co-glycolic acid) (mPEG-PLGA) using the solvent-diffusion technique. The obtained ABG-PNs were 105 nm in size with a small polydispersity index of 0.08. The entrapment efficiency and drug loading were 71.9% and 4.58%, respectively. Cellular uptake of ABG-PNs was controlled by specific clathrin-mediated endocytosis. In addition, ABG-PNs showed improved drug pharmacokinetics with an increased area under the curve value (a 1.73-fold increase) and a decreased elimination clearance (37.8% decrease). The nanomicelles showed increased drug concentrations in the liver and lung. In contrast, drug concentrations in both heart and brain were decreased. Moreover, the nanomicelles enhanced the anticancer effect of the pure drug probably via increased cellular uptake of drug molecules. In conclusion, the mPEG-PLGA-based nanomicelle system is a satisfactory carrier for the systemic delivery of ABG.

**Keywords:** bufanolide steroid, arenobufagin, nanomicelles, mPEG-PLGA

Introduction

Arenobufagin (ABG) (Figure 1) is a bufanolide steroid derived from the venom of giant toads (eg, *Bufo gargarizans* and *Bufo melanostictus* Schneider). Toad venom is well known as a Chinese traditional medicine and typically used for the treatment of liver cancer.[1,2] Recent studies have indicated that bufanolide steroids (eg, bufalin, cinobufagin, and ABG) are responsible for the anticancer effects of toad venom because this type of steroid shows strong antitumor activities.[3–5] Of note, ABG perhaps is the most potent antitumor ingredient.[6] The antitumor mechanisms of ABG appear to be multifaceted. It inhibits tumor growth through interference with mechanistic target of rapamycin, vascular endothelial growth factor receptor-2, and/or ATM/ATR signaling pathways.[5,7,8] In addition, ABG functions as a potent Na⁺-K⁺ pump inhibitor and thus has great potential in the management of heart diseases.[9] However, poor solubility of ABG poses a challenge to in vivo pharmacological studies due to drug delivery difficulties. There is a clear need to find a suitable method to resolve the drug delivery problem of ABG.

Various delivery systems (formulation strategies), including liposomes,[10] micelles,[11] and microemulsions,[12] have been adopted to improve the solubility of drugs. Of these delivery systems, polymeric micelles receive enormous attention due to significant
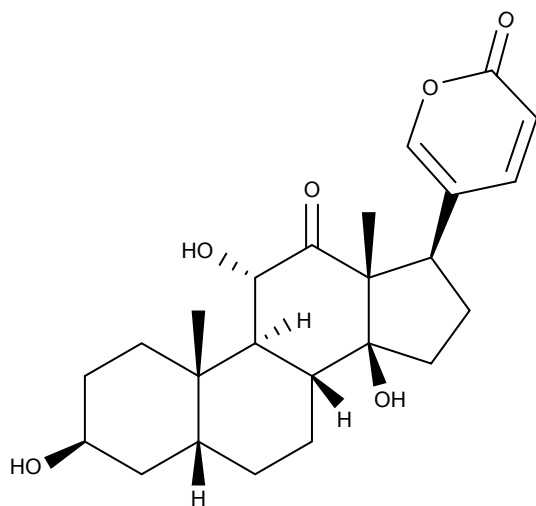
Figure 1 Chemical structure of arenobufagin.

advantages (eg, superior storage stability, excellent tissue permeability, and outstanding biocompatibility).[13] Polymeric micelles are a type of nano-sized drug carrier self-assembled in aqueous medium from amphiphilic block copolymers.[13,14] By forming a hydrophobic core, the polymeric micelles possess great ability to increase the aqueous solubility of insoluble (hydrophobic) drugs. Compared to the micelles made of low molecular weight surfactants, polymeric micelles are more advantageous in drug solubilization applications because of the low toxicity of neutral polymers.[15]

Methoxy poly (ethylene glycol)-block-poly (D,L-lactic-co-glycolic acid) (mPEG-PLGA) is a amphiphilic block copolymer frequently used in the preparation of polymeric micelles.[16] Both mPEG and PLGA are nontoxic and non-immunogenic polymers that have been approved by the Food and Drug Administration for human uses.[17] mPEG-based polymeric micelles tend to have a prolonged blood residence time because of reduced phagocytosis by the reticuloendothelial system (RES).[18] In addition to the passive targeting feature, mPEG-PLGA micelles show preferential accumulation in tumors and at sites of inflammations due to the enhanced vascular permeability and retention (EPR) effect.[19,20] Sodium oleate is regarded as a safe pharmaceutical excipient and has been approved as an injectable ingredient in China.[11] Inclusion of sodium oleate would help to stabilize the physical stability of micelles and to improve drug loading (DL).[21]

Although ABG shows excellent anticancer effects, the development of ABG as a therapeutic agent is significantly limited by the poor solubility. In this study, we aimed to explore the potential of polymeric micelles in the systemic delivery of ABG. ABG-loaded polymeric nanomicelles

(ABG-PNs) were prepared with mPEG-PLGA using the solvent-diffusion technique. Prepared micelles were characterized by particle size, morphology, entrapment efficiency (EE), and drug release in vitro. Cellular uptake mechanism and anticancer effect of ABG-PNs were determined using HepG2 cells. Pharmacokinetic and tissue distribution studies of ABG-PNs were performed with Sprague Dawley rats. We demonstrated for the first time that mPEG-PLGA-based nanomicelles were a satisfactory carrier for the systemic delivery of ABG.

Materials and methods
Materials
ABG was purchased from Baoji Herbest Bio-Tech Co, Ltd (Shanxi, China). mPEG (M_n =3,400)-block-PLGA (75/25, M_n =10,000) was purchased from RuiXi Bio-Tech Co, Ltd (Xi'an, China). Sodium oleate, sucrose, chlorpromazine, simvastatin, ethylisopropyl amiloride (EIPA), filipin, and latrunculin B were obtained from Sigma Aldrich Co. (St Louis, MO, USA). High performance liquid chromatography (HPLC)-grade acetonitrile was obtained from Mreda Technology Inc. (MA, USA). All other chemicals were of analytical grade and used as received.

Preparation of ABG-PNs
ABG-PNs were prepared using the solvent-diffusion technique. In brief, fixed amounts of mPEG-PLGA and ABG were dissolved in 1 mL of 80% ethanol solution (v/v). The resulting mixture was rapidly injected into 5 or 10 mL of 0.5% sodium oleate with a syringe under magnetic stirring (0.5, 2, or 5 hours), generating the micelles. The residual ethanol was removed by a rotatory evaporator (under a low pressure at 30°C).

Measurement of particle size
The particle size of ABG-PNs was determined by dynamic light scattering using Zetasizer Nano ZS (Malvern Instruments, Malvern, UK) as described.[22] In brief, a 20-μL aliquot of ABG-PNs was diluted with deionized water to a final volume of 1 mL, and then subjected to laser diffraction. The data were analyzed with the build-in software for the output of particle size based on dynamic light scattering.

Determination of EE and DL
EE and DL were determined using the ultrafiltration method. In brief, 400 μL of micelle preparation was added into the centrifugal filter device (Amicon Ultra-0.5, MW =10 k; Millipore, MA, USA), followed by centrifugation at 10,000 *g*

for 10 minutes. The ultrafiltrate was collected and subjected to HPLC analysis for drug quantification (to obtain free drug concentration [C_{free}]). Total drug concentration (C_{total}) was derived as the ratio of the amount of drug added versus the total volume (V) of the preparation. EE and DL values were calculated according to the following formulas.

$$EE\ (\%) = \frac{C_{total} - C_{free}}{C_{total}} \times 100$$

$$DL\ (\%) = \frac{(C_{total} - C_{free}) \times V}{Total\ amounts\ of\ added\ drug\ and\ excipients} \times 100$$

Surface morphology

Morphology examination of ABG-PNs was performed using transmission electron microscopy (TEM; JEM-1230; JEOL, Tokyo, Japan) as previously described.[23] In brief, an aliquot of ABG-PNs was placed on a carbon-coated copper grid and allowed to dry at room temperature. Once dried, the sample was subjected to TEM inspection.

Drug release study

Drug release study was performed using a dialysis technique as described earlier.[24] In brief, 1 mL sample was transferred into dialysis bags (molecular weight cutoff =10 kd), followed by ligation with silk ties. Phosphate buffer solution (PBS, pH =7.4, 100 mL) maintained at 37°C was used as the release medium under magnetic stirring. At each specified time point, 0.2 mL of dialysate was withdrawn and replenished with the same volume of fresh release medium. The concentrations of ABG were measured by HPLC. The release curve was plotted with cumulative drug release as the function of time.

Anticancer activity measurement

Cytotoxicity tests were performed using HepG2 cells (Cell Bank of Chinese Academy of Sciences, Shanghai, China). In brief, the cells were seeded in a 96-well plate and cultured in Dulbecco's Modified Eagle's Medium (DMEM) supplemented with 10% fetal bovine serum (FBS). On the next day, a series of concentrations of ABG-PNs were added into the culture wells. After 48-hour incubation, the cells were subjected to MTT assays as previously described.[25] Optical density measurements were performed at 570 nm using a Synergy HTX microplate reader (Biotek, Winooski, VT, USA).

Cellular uptake study

Cellular uptake mechanism of ABG-PNs was determined using HepG2 cells (Cell Bank of Chinese Academy of Sciences). Cells were seeded in 6-well plates at a density of 4.0×10^5 cells/well and cultured in DMEM supplemented with 10% FBS. On the next day, the culture medium was replaced with serum-free medium containing 5 µg/mL ABG-PNs. After incubation for 1, 2, or 4 hours, the medium was removed and the cells were washed with ice-cold PBS twice. The cells were lysed with 400 µL of radioimmunoprecipitation assay lysis buffer (0.1% phenylmethylsulfonyl fluoride), followed by centrifugation at 12,000 g for 15 minutes. A 2-µL aliquot of the supernatant was collected for measurement of the total protein concentration with a BCA Protein Assay Kit. The remaining supernatant was mixed well with 200 µL of 50% acetonitrile, followed by ultrasonication for 20 minutes and centrifugation at 13,000 g for 10 minutes; the resulting supernatant was collected and subjected to ultra performance liquid chromatography (UPLC)-mass spectrometry (MS)/quadrupole time of flight (QTOF) analysis for ABG quantification.

To determine the cellular uptake mechanisms, HepG2 cells were pretreated with each of the endocytosis inhibitors (ie, 0.5 M hypertonic sucrose, 25 µM chlorpromazine, 25 µM simvastatin, 50 µM EIPA, 1 µM filipin, and 15 mM latrunculin B) for 0.5 hours. The cells were then incubated with ABG-PNs for 4 hours at 37°C. At the end of the experiments, the cells were collected and processed to determine intracellular ABG by UPLC-MS/QTOF analysis. To determine the effect of temperature on nanomicelle uptake, the cells were maintained at 37°C for 0.5 hours, and then incubated with ABG-PNs at 4°C for 4 hours. At the end of the experiment, the cells were collected and processed to determine intracellular ABG.

Pharmacokinetic study

All animal experiments were conducted according to the Guidelines on the Care and Use of Animals for Scientific Purposes (2004). The protocols for the animal studies were also reviewed and approved by the Experimental Animal Ethical Committee of Jinan University. Pharmacokinetic study was performed with jugular vein-cannulated Sprague Dawley rats (male, 190–210 g). These rats were randomly divided into two groups (n=5 per group), namely, the control and treatment groups. Control group received ABG cosolvent (water:ethanol:PEG400 =78:20:2) at a dose of 3.5 mg/kg by bolus injection via the jugular vein, whereas the treatment group received ABG-PNs at the same dose.

Blood samples were collected via the jugular vein at 5, 15, 30, 45, 60, 90, 120, 240, 360, and 480 minutes after drug administration, and subjected to centrifugation at 5,000 g for 8 minutes. The resulting plasma samples were stored at $-80°C$ until analysis.

For preparation of analytical samples, 0.5 mL acetonitrile containing 0.25 µM SNX-2112 (internal standard) was added to 0.1 mL plasma sample to precipitate proteins. The mixture was vortexed for 3 minutes, and then centrifuged at 13,000 g for 10 minutes. The supernatant was transferred to a new centrifuge tube, followed by sample drying using Eppendorf Concentrator Plus (Hamburg, Germany). The dry residuals were reconstituted in 100 µL of 50% acetonitrile. After centrifugation (13,000 g, 15 minutes), a 5-µL aliquot of the supernatant was injected into the UPLC-QTOF/MS system.

Tissue distribution determination

Male Sprague Dawley rats (190–210 g) were randomly divided into two groups, namely, the control and treatment groups (n=12 per group). Control group received ABG cosolvent (water:ethanol:PEG400 =78:20:2) at a dose of 3.5 mg/kg by bolus injection via the jugular vein, whereas the treatment group received ABG-PNs at the same dose. At each time point (0.5, 2, and 4 hours), four rats were rendered unconscious for tissue sampling by injecting chloral hydrate. After washout of blood with ice-cold saline, the brain, heart, liver, spleen, lung, and kidney were rapidly removed, weighed, and stored at $-80°C$.

The tissues were defrozen and homogenized at a ratio of 1/2 (w/v) in saline solution. The homogenate was mixed with acetonitrile containing the internal standard SNX-2112. This mixture was subjected to vortexing for 3 minutes and 13,000 g centrifugation at 4°C for 10 minutes. The supernatant was collected and dried using Eppendorf Concentrator Plus. The dry residues were reconstituted in 100 µL of 50% acetonitrile. After centrifugation (13,000 g, 15 minutes), the supernatant was subjected to UPLC-QTOF/MS analysis.

Quantification of ABG

The concentrations of ABG in in vitro release samples were determined using a Dionex UltiMate 3000 HPLC system (Thermo Fisher Scientific, Waltham, MA, USA) equipped with a quaternary pump, a degasser, an autosampler, a column heater, and a multichannel rapid scanning UV–VIS detector. Chromatographic separation was performed on a Thermo Acclaim 120 C18 column (4.6×250 mm, 5 µm; maintained at 40°C) with isocratic elution (40% acetonitrile as the mobile

phase) at a flow rate of 1.0 mL/min. The injection volume was 10 µL and the wavelength of detection was 299 nm.

The concentrations of ABG in cell and biological samples were quantified using a UPLC-QTOF/MS system consisting of Waters ACQUITY UPLC and Xevo G2 QTOF/MS (Waters Corporation, Milford, MA, USA). Chromatographic separation was performed on a BEH column (2.1×50 mm, 1.7 µm; Waters Corporation) with a gradient elution of formic acid (0.1%) in water (mobile phase A) versus formic acid (0.1%) in acetonitrile (mobile phase B). The flow rate was set at 0.25 mL/min. The gradient program consisted of 10% B at 0–0.5 minutes, 10%–80% B at 0.5–3.0 minutes, 80% B at 3.0–3.5 minutes, and 80%–10% B at 3.5–4.0 minutes. QTOF mass spectrometer was operated at the positive ion scan mode and the other parameter settings have been described in our previous publication.[26]

Data analysis

Data are presented as mean ± SD (for in vitro data) and mean ± SEM (for in vivo data). Pharmacokinetic modeling was performed using the WinNonlin software version 6.3 (Pharsight, Mountain View, CA, USA). Statistically significant differences were analyzed by Student's t-test. The level of significance was set at $P < 0.05$.

Results
Preparation and characterization of ABG-PNs

We assessed the effects of formulation variables (including the amount ratio of drug over polymer, the volume ratio of the aqueous over organic phase, and the stirring time) on the formation of ABG-PNs (Table 1). The formulation variables at tested levels showed a minor effect on the particle size (~100–130 nm). However, the EE was the highest when the amount ratio of drug over polymer was 1:6 (Table 1). Also, there was a general tendency that the EE increased as both the volume ratio of the aqueous over organic phase and the stirring time increased (Table 1). In contrast, DL decreased with the volume ratio of the aqueous over organic phase, but increased as the stirring time increased (Table 1). Taken together, the optimal formula for ABG-PNs was defined as follows: the amount ratio of drug over polymer, 1:6; the volume ratio of the aqueous over organic phase, 5:1, and the stirring time, 5 hours. The obtained ABG-PNs were 105.4 nm in size with a small polydispersity index of 0.08 (Figure 2A). The TEM image showed that ABG-PNs were spherical or nearly spherical (Figure 2B). The drug release profile of ABG-PNs was comparable to that of the control cosolvent

Table I Effects of formulation variables on the particle size, EE, and DL of ABG-PNs

Formulation	Amount ratio of drug over polymer	Volume ratio of the aqueous over organic phase	Stirring time (h)	Size distribution (nm)	EE (%)	DL (%)
F1	1:4	10:1	0.5	98.9±4.96	36.1±1.32	3.96±0.14
F2	1:6	10:1	0.5	116±4.52	56.4±2.36	3.15±0.13
F3	1:8	10:1	0.5	110±3.30	32.5±1.61	2.43±0.12
F4	1:6	2.5:1	0.5	121±7.23	46.1±1.26	4.92±0.13
F5	1:6	5:1	0.5	103±5.23	46.7±2.03	3.82±0.16
F6	1:6	10:1	0.5	116±4.52	56.4±2.36	3.15±0.13
F7	1:6	10:1	0.5	116±4.52	56.4±2.36	3.15±0.13
F8	1:6	10:1	2	138±6.23	68.0±3.28	4.33±0.21
F9	1:6	10:1	5	109±3.55	71.9±3.41	4.58±0.22

Abbreviations: ABG, arenobufagin; PNs, polymeric nanomicelles; EE, entrapment efficiency; DL, drug loading.

formulation (similarity factor f_1 =75.7, Figure 3), suggestive of significantly enhanced dissolution. Also, ABG was rapidly released from the nanomicelles as indicated by up to 90% of the drug dissolved within 2 hours (Figure 3).

Cellular uptake mechanism

Uptake of ABG (in both cosolvent and nanomicelle forms) to HepG2 cells increased as a function of time (Figure 4). As expected, the cellular uptake of ABG was significantly higher in nanomicelle (ABG-PNs) than in the cosolvent group (Figure 4). The results suggested that ABG-PNs could enhance the delivery of ABG into cells.

Six endocytosis inhibitors were used to determine the mechanisms underlying cellular uptake of ABG-PNs (Figure 5). Of these, hypertonic sucrose and chlorpromazine are respective inhibitors of nonspecific and specific clathrin-dependent endocytosis; simvastatin and filipin are respective inhibitors of nonspecific and specific caveolae-dependent endocytosis; and EIPA and latrunculin B are respective inhibitors of macropinocytosis-dependent and phagocytosis-dependent endocytosis. Only chlorpromazine caused an altered (reduced) drug uptake ($P<0.05$) (Figure 5), suggesting that specific clathrin- dependent endocytosis was responsible for the cellular uptake of ABG-PNs. This active

(energy-dependent) uptake mechanism was also supported by the fact that cellular uptake of ABG was significantly suppressed by a decreased temperature (Figure 5).

Pharmacokinetic characterization

The plasma concentrations of ABG versus time profiles were determined in rats after administration of ABG-PNs or ABG cosolvent (Figure 6). Compared to the cosolvent, the nanomicelles showed significantly higher plasma drug concentrations at all time points except for 5 and 360 minutes (Figure 6). The pharmacokinetic data were best fitted by the two-compartment model (Table 2). The area under the curve $(AUC)_{0-8h}$ of ABG-PNs was 1.73 times that of the cosolvent (54.9 vs 95.1 mg/mL/min, $P<0.05$), consistent with elevated drug plasma concentrations. In addition, the nanomicelles showed a decreased elimination clearance value compared to the control cosolvent (26.7 vs 42.9 mL/kg/min, $P<0.05$). The results suggested that enhanced drug exposure by ABG-PNs may be associated with reduced body clearance.

Tissue distribution

After administration of each of the ABG formulations, ABG was found in major tissues including the heart, liver, spleen, lung, kidney, and brain (Figure 7). In general, the
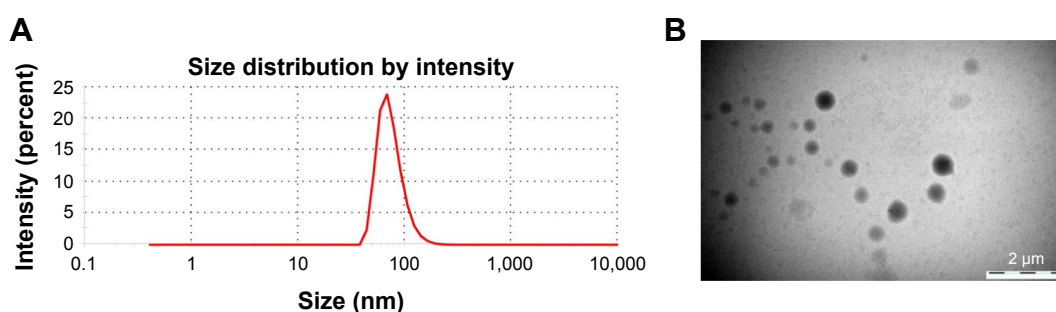
Figure 2 Characterization of ABG-PNs.
Notes: (**A**) Particle size distribution; (**B**) TEM micrograph.
Abbreviations: ABG, arenobufagin; PNs, polymeric nanomicelles; TEM, transmission electron microscopy.
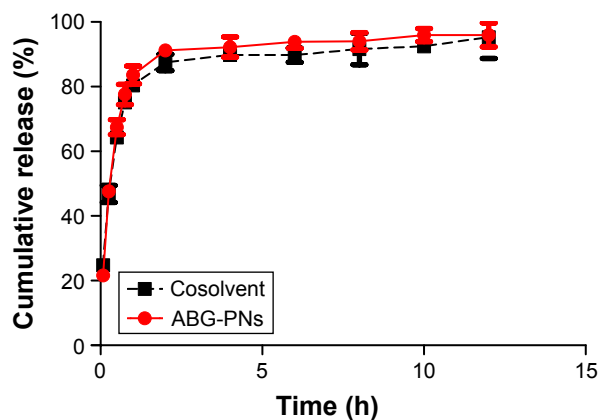
Figure 3 In vitro cumulative ABG release from the cosolvent and ABG-PNs in PBS (pH =7.4).
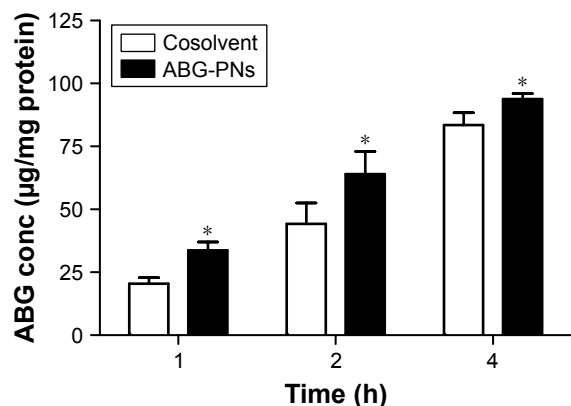**Note:** Data are expressed as mean ± SD (n=3).
Abbreviations: ABG, arenobufagin; PNs, polymeric nanomicelles; PBS, phosphate buffer solution; SD, standard deviation.

ABG levels in all tissues decreased as a function of time (Figure 7). Compared to the cosolvent, nanomicelles showed significantly increased or unchanged drug concentrations in the liver and lung depending on the sampling time (Figure 7). In contrast, drug concentrations in both the heart and brain were significantly decreased or unaltered (depending on the sampling time) by nanomicelles (Figure 7). Further, there were no differences in the spleen and kidney concentrations between nanomicelles and the cosolvent (Figure 7).

## Anticancer activity measurement

The anticancer effects of ABG-PNs were assessed with HepG2 cells and MTT assays. We confirmed that blank micelles showed no effects on the cells (data not shown).

Figure 4 Cellular uptake study of ABG-PNs.
Notes: ABG accumulation in HepG2 cells at different time points was determined by UPLC-QTOF/MS. Data are expressed as mean ± SD (n=3). Significant differences were marked as *$P<0.05$.
Abbreviations: ABG, arenobufagin; PNs, polymeric nanomicelles; SD, standard deviation; UPLC, ultra performance liquid chromatography; QTOF, quadrupole time of flight; MS, mass spectrometry; conc, concentration.
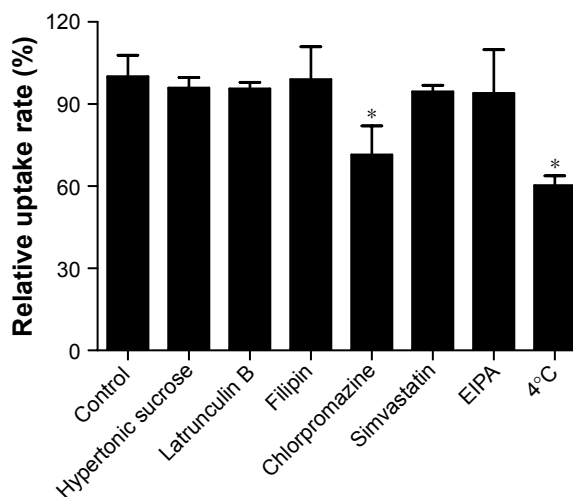
Figure 5 Modulatory effects of endocytosis inhibitors and temperature on uptake of ABG-PNs by HepG2 cells.
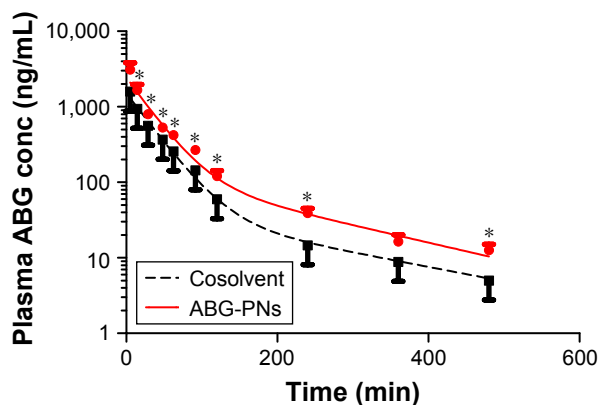**Notes:** *$P<0.05$ versus control. Data are expressed as mean ± SD (n=3).
Abbreviations: ABG, arenobufagin; PNs, polymeric nanomicelles; SD, standard deviation; EIPA, ethylisopropyl amiloride.

As expected, pure ABG (an anticancer agent) demonstrated a cytotoxic effect with a half maximal inhibitory concentration (IC_{50}) value of 0.32 μM (Figure 8). Interestingly, the nanomicelles appeared to significantly enhance the cytotoxic effect of ABG with a smaller IC_{50} value of 0.14 μM (Figure 8). The enhanced anticancer effect of nanomicelles may be attributed to elevated drug accumulation within the cells (Figure 4).

Discussion

Systemic delivery of ABG, a promising anticancer agent, is challenged by its poor aqueous solubility. In this study, we developed and characterized an mPEG-PLGA-based

Figure 6 Plasma ABG concentrations versus time curves for drug cosolvent and ABG-PNs in rats at a dose of 3.5 mg/kg.
Notes: Data are expressed as mean ± SEM (n=5). *$P<0.05$ versus control.
Abbreviations: ABG, arenobufagin; PNs, polymeric nanomicelles; SEM, standard error of means; conc, concentration.

Table 2 List of pharmacokinetic parameters derived by fitting the conventional two-compartment model to the plasma data

Parameter	Unit	ABG-SOL	SEM	ABG-PNs	SEM
K_{10}	1/h	1.68	0.15	1.86	0.27
K_{12}	1/h	0.28	0.25	0.58	0.23
K_{21}	1/h	0.31	0.04	0.56	0.09
$t_{1/2alpha}$	min	21.5	1.80	18.3	2.78
$t_{1/2beta}$	min	179	32.6	108	12.8
CL	mL/kg/min	42.9	1.89	26.7*	3.04
CL_2	mL/kg/min	7.2	0.72	6.76	1.52
AUC_{0-t}	mg/mL/min	54.9	2.71	95.1*	15.1

Note: Significant differences between drug cosolvent and ABG-PNs were marked as *$P<0.05$.
Abbreviations: ABG, arenobufagin; PNs, polymeric nanomicelles; SEM, standard error of means; AUC, area under the curve; SOL, cosolvent; CL, clearance.

nanomicelle system for ABG (ie, ABG-PNs). ABG-PNs facilitated systemic delivery of ABG through a marked increase in the aqueous solubility. In addition, ABG-PNs showed improved drug pharmacokinetics with an increased AUC value (Figure 6). Moreover, the nanomicelles enhanced the anticancer effect of the pure drug probably via increased cellular uptake of drug molecules (Figure 8).

The mPEG-PLGA copolymer was selected to formulate the nanomicelles for ABG. This was because mPEG-PLGA-based micelles usually have high physical stability with or without dilution due to a low critical micelle concentration value of the copolymer.[27,28] Drug release from ABG-PNs was rapid and comparable to that from the cosolvent formulation (Figure 3), supporting that the PNs rapidly dissolved in the medium upon dilution. Sodium oleate was included in the formula to improve the DL because micelles consisting of

fatty acids generally show a high ability to solubilize drugs.[29] Screening experiments identified three formulation variables (ie, the amount ratio of drug over polymer, the volume ratio of the aqueous over organic phase, and the stirring time) contributing to variations in EE and DL (Table 1). An optimal formulation was finalized by taking into consideration reasonable high values of both EE and DL. The optimized nanomicelles showed a desired particle size (nano-sized), drug concentration (3.5 mg/mL, sufficient for systemic delivery), and physical stability (stable for up to 1 month, data not shown).

ABG-PNs showed superior anticancer effect compared to the cosolvent formulation. The IC_{50} value of ABG-PNs for killing HepG2 cells was significantly lower than that of the cosolvent (Figure 8). This is most likely due to the increased cellular uptake of ABG-PNs (Figure 4). Cellular uptake of ABG-PNs was controlled by the specific clathrin-dependent endocytosis, revealed by the chemical inhibition studies (Figure 5). This uptake mechanism was evidenced by the fact that cellular uptake of ABG was significantly suppressed when cells were cultured at 4°C (Figure 5). At a low temperature, the adenosine triphosphate (ATP) output is limited due to the activity inhibition of energy-productive enzymes, resulting in a reduction of cellular uptake.[25,30] Endocytosis generally is a more efficient uptake process than others such as passive diffusion and carrier-mediated transport.[31,32]

ABG-PNs showed an improved pharmacokinetic profile that was featured with an increase in AUC value and a decrease in body clearance (Figure 6). The altered pharmacokinetics was attributed to good physical stability and stealth
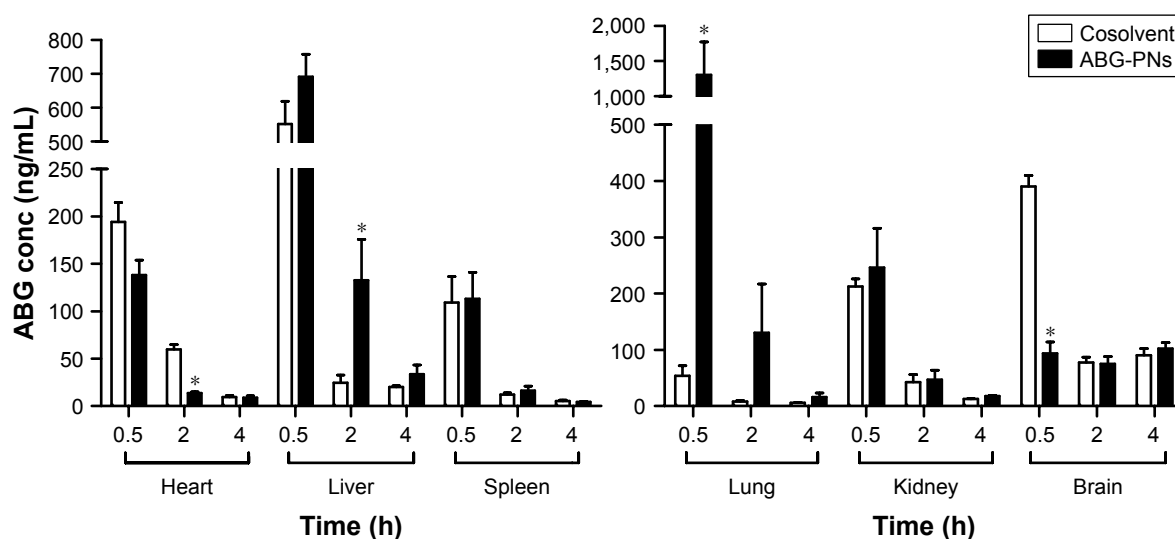
Figure 7 Tissue distribution of ABG after intravenous administration of cosolvent and ABG-PNs (at a dose of 3.5 mg/kg) at 0.5, 2, and 4 hours.
Notes: Data are expressed as mean ± SEM (n=4). *$P<0.05$ versus control.
Abbreviations: ABG, arenobufagin; PNs, polymeric nanomicelles; SEM, standard error of means; conc, concentration.
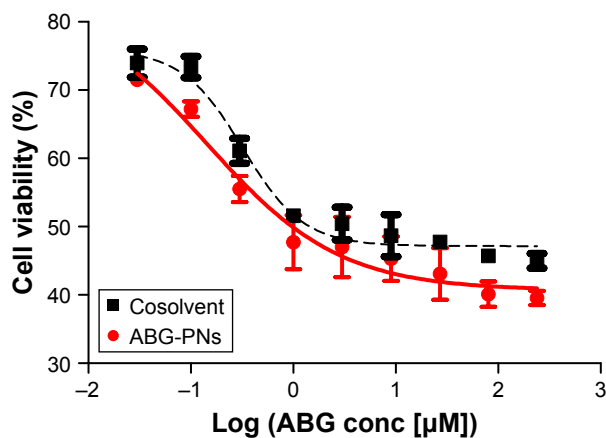
Figure 8 Anticancer activity measurement of drug cosolvent and ABG-PNs using HepG2 cell line.
Abbreviations: ABG, arenobufagin; PNs, polymeric nanomicelles; conc, concentration.

effect of pegylated nanomicelles.[33,34] The nano-sized micelles led to increased drug accumulation in RES-enriched tissues such as the liver and lung (Figure 7). This surely will be a great benefit when the compound is used for the treatment of liver and lung cancers. In addition, due to the small size (10 nm–2 μm), the nanomicelles may provide efficient passive tumor-targeting ability through EPR effect.[35,36]

Recent studies have shown that ABG (bearing a similar chemical structure to cardiac glycoside drugs) has cardiac toxicity due to unwanted accumulation of the drug in the heart.[9,37] In this regard, our ABG-PNs have a significant advantage, namely, reduced cardiac toxicity, because drug distribution was lowered in the heart by administration of the nanomicelles.[21,38,39] Furthermore, we observed a decreased level of ABG in the brain for ABG-PNs dosing, again highlighting that altered drug tissue distribution by the nano-carriers may contribute to minimal side effects.

In summary, we prepared and characterized a polymeric micelles system for ABG (ABG-PNs). ABG-PNs facilitated systemic delivery of ABG through a marked increase in the aqueous solubility. In addition, ABG-PNs showed improved drug pharmacokinetics with an increased AUC value. Moreover, the nanomicelles enhanced the anticancer effect probably via increased cellular uptake of drug molecules. It is concluded that PNs are a satisfactory carrier for the systemic delivery of ABG.

Acknowledgments

Disclosure

The authors report no conflicts of interest in this work.

References

1. Yang Q, Zhou X, Zhang M, et al. Angel of human health: current research updates in toad medicine. *Am J Transl Res*. 2015;7:1–14.
2. Meng Q, Yau LF, Lu JG, et al. Chemical profiling and cytotoxicity assay of bufadienolides in toad venom and toad skin. *J Ethnopharmacol*. 2016;187:74–82.
3. Moreno YBL, Urban E, Gelbcke M, et al. Structure–activity relationship analysis of bufadienolide-induced in vitro growth inhibitory effects on mouse and human cancer cells. *J Nat Prod*. 2013;76:1078–1084.
4. Baek SH, Kim C, Lee JH, et al. Cinobufagin exerts anti-proliferative and pro-apoptotic effects through the modulation ROS-mediated MAPKs signaling pathway. *Immunopharmacol Immunotoxicol*. 2015; 37:265–273.
5. Li M, Wu S, Liu Z, et al. Arenobufagin, a bufadienolide compound from toad venom, inhibits VEGF-mediated angiogenesis through suppression of VEGFR-2 signaling pathway. *Biochem Pharmacol*. 2012;83: 1251–1260.
6. Han L, Wang H, Si N, et al. Metabolites profiling of 10 bufadienolides in human liver microsomes and their cytotoxicity variation in HepG2 cell. *Anal Bioanal Chem*. 2016;408:2485–2495.
7. Zhang DM, Liu JS, Deng LJ, et al. Arenobufagin, a natural bufadienolide from toad venom, induces apoptosis and autophagy in human hepatocellular carcinoma cells through inhibition of PI3K/Akt/mTOR pathway. *Carcinogenesis*. 2013;34:1331–1342.
8. Deng LJ, Peng QL, Wang LH, et al. Arenobufagin intercalates with DNA leading to G2 cell cycle arrest via ATM/ATR pathway. *Oncotarget*. 2015;6:34258–34275.
9. Cruz Jdos S, Matsuda H. Arenobufagin, a compound in toad venom, blocks Na(+)-K+ pump current in cardiac myocytes. *Eur J Pharmacol*. 1993;239:223–226.
10. Mohammed AR, Weston N, Coombes AG, Fitzgerald M, Perrie Y. Liposome formulation of poorly water soluble drugs: optimisation of drug loading and ESEM analysis of stability. *Int J Pharm*. 2004;285: 23–34.
11. Ishihara T, Goto M, Kanazawa H, Higaki M, Mizushima Y. Efficient entrapment of poorly water-soluble pharmaceuticals in hybrid nanoparticles. *J Pharm Sci*. 2009;98:2357–2363.
12. He CX, He ZG, Gao JQ. Microemulsions as drug delivery systems to improve the solubility and the bioavailability of poorly water-soluble drugs. *Expert Opin Drug Deliv*. 2010;7:445–460.
13. Letchford K, Burt H. A review of the formation and classification of amphiphilic block copolymer nanoparticulate structures: micelles, nanospheres, nanocapsules and polymersomes. *Eur J Pharm Biopharm*. 2007;65:259–269.
14. Jeetah R, Bhaw-Luximon A, Jhurry D. Polymeric nanomicelles for sustained delivery of anti-cancer drugs. *Mutat Res*. 2014;768:47–59.
15. Haag R, Kratz F. Polymer therapeutics: concepts and applications. *Angew Chem Int Ed Engl*. 2006;45:1198–1215.
16. Wang H, Zhao Y, Wu Y, et al. Enhanced anti-tumor efficacy by co-delivery of doxorubicin and paclitaxel with amphiphilic methoxy PEG-PLGA copolymer nanoparticles. *Biomaterials*. 2011;32:8281–8290.
17. Lu JM, Wang X, Marin-Muller C, et al. Current advances in research and clinical applications of PLGA-based nanotechnology. *Expert Rev Mol Diagn*. 2009;9:325–341.
18. Alexis F, Pridgen E, Molnar LK, Farokhzad OC. Factors affecting the clearance and biodistribution of polymeric nanoparticles. *Mol Pharm*. 2008;5:505–515.
19. Nishiyama N, Okazaki S, Cabral H, et al. Novel cisplatin-incorporated polymeric micelles can eradicate solid tumors in mice. *Cancer Res*. 2003;63:8977–8983.

20. Matsumura Y, Maeda H. A new concept for macromolecular therapeutics in cancer chemotherapy: mechanism of tumoritropic accumulation of proteins and the antitumor agent smancs. *Cancer Res*. 1986;46:6387–6392.

21. Zhang T, Wang H, Ye Y, Zhang X, Wu B. Micellar emulsions composed of mPEG-PCL/MCT as novel nanocarriers for systemic delivery of genistein: a comparative study with micelles. *Int J Nanomedicine*. 2015;10:6175–6184.

22. Li W, Zhang T, Ye Y, Zhang X, Wu B. Enhanced bioavailability of tripterine through lipid nanoparticles using broccoli-derived lipids as a carrier material. *Int J Pharm*. 2015;495:948–955.

23. Zhang X, Chen G, Zhang T, Ma Z, Wu B. Effects of PEGylated lipid nanoparticles on the oral absorption of one BCS II drug: a mechanistic investigation. *Int J Nanomedicine*. 2014;9:5503–5514.

24. Zhou X, Zhang X, Ye Y, et al. Nanostructured lipid carriers used for oral delivery of oridonin: an effect of ligand modification on absorption. *Int J Pharm*. 2015;479:391–398.

25. Dong D, Quan E, Yuan X, Xie Q, Li Z, Wu B. Sodium oleate-based nanoemulsion enhances oral absorption of chrysin through inhibition of UGT-mediated metabolism. *Mol Pharm*. Epub 2016 Dec 16.

26. Dong D, Sun H, Wu ZF, Wu BJ, Xue YX, Li ZJ. A validated ultra-performance liquid chromatography-tandem mass spectrometry method to identify the pharmacokinetics of SR8278 in normal and streptozotocin-induced diabetic rats. *J Chromatogr B Analyt Technol Biomed Life Sci*. 2016;1020:142–147.

27. Peng KT, Chen CF, Chu IM, et al. Treatment of osteomyelitis with teicoplanin-encapsulated biodegradable thermosensitive hydrogel nanoparticles. *Biomaterials*. 2010;31:5227–5236.

28. Li T, Ci T, Chen L, Yu L, Ding J. Salt-induced reentrant hydrogel of poly(ethylene glycol)–poly(lactide-co-glycolide) block copolymers. *Polym Chem*. 2014;5:979–991.

29. Lu Y, Park K. Polymeric micelles and alternative nanonized delivery vehicles for poorly soluble drugs. *Int J Pharm*. 2013;453:198–214.

30. Zhang X, Zhang T, Ye Y, et al. Phospholipid-stabilized mesoporous carbon nanospheres as versatile carriers for systemic delivery of amphiphobic SNX-2112 (a Hsp90 inhibitor) with enhanced antitumor effect. *Eur J Pharm Biopharm*. 2015;94:30–41.

31. Yakubov LA, Deeva EA, Zarytova VF, et al. Mechanism of oligonucleotide uptake by cells: involvement of specific receptors? *Proc Natl Acad Sci U S A*. 1989;86:6454–6458.

32. Oh JM, Choi SJ, Kim ST, Choy JH. Cellular uptake mechanism of an inorganic nanovehicle and its drug conjugates: enhanced efficacy due to clathrin-mediated endocytosis. *Bioconjug Chem*. 2006;17:1411–1417.

33. Guo J, Gao X, Su L, et al. Aptamer-functionalized PEG-PLGA nanoparticles for enhanced anti-glioma drug delivery. *Biomaterials*. 2011;32:8010–8020.

34. Bearinger JP, Terrettaz S, Michel R, et al. Chemisorbed poly(propylene sulphide)-based copolymers resist biomolecular interactions. *Nat Mater*. 2003;2:259–264.

35. van Vlerken LE, Amiji MM. Multi-functional polymeric nanoparticles for tumour-targeted drug delivery. *Expert Opin Drug Deliv*. 2006;3:205–216.

36. Nasongkla N, Bey E, Ren J, et al. Multifunctional polymeric micelles as cancer-targeted, MRI-ultrasensitive drug delivery systems. *Nano Lett*. 2006;6:2427–2430.

37. Cruz Jdos S, Matsuda H. Depressive effects of arenobufagin on the delayed rectifier K+ current of guinea-pig cardiac myocytes. *Eur J Pharmacol*. 1994;266:317–325.

38. Takahashi A, Yamamoto Y, Yasunaga M, et al. NC-6300, an epirubicin-incorporating micelle, extends the antitumor effect and reduces the cardiotoxicity of epirubicin. *Cancer Sci*. 2013;104:920–925.

39. Maciel NR, Reis PG, Kato KC, et al. Reduced cardiovascular alterations of tartar emetic administered in long-circulating liposomes in rats. *Toxicol Lett*. 2010;199:234–238.